Journal of Physiology - Paris 103 (2009) 315–323

Contents lists available at ScienceDirect

Journal of Physiology - Paris

journal homepage: www.elsevier.com/locate/jphysparis

Brain signal analysis based on recurrences

Stefan Schinkel [a,*], Norbert Marwan [a,b], Jürgen Kurths [b,c]

[a] Interdisciplinary Centre for Dynamics of Complex Systems, University of Potsdam, Am Neuen Palais 10, 14469 Potsdam, Germany
[b] Potsdam-Institut für Klimafolgenforschung e.v., Po box 601203, 14412 Potsdam, Germany
[c] Humboldt Universität zu Berlin, Institut für Physik, Newtonstr. 15, 12489 Berlin, Germany

ARTICLE INFO

Keywords:
EEG
ERP
RP
RQA
Order patterns
N400

ABSTRACT

The EEG is one of the most commonly used tools in brain research. Though of high relevance in research, the data obtained is very noisy and nonstationary. In the present article we investigate the applicability of a nonlinear data analysis method, the recurrence quantification analysis (RQA), to such data. The method solely rests on the natural property of recurrence which is a phenomenon inherent to complex systems, such as the brain. We show that this method is indeed suitable for the analysis of EEG data and that it might improve contemporary EEG analysis.

1. Introduction

Recurrence is a fundamental property of complex dynamical systems (Marwan et al., 2007) and the human brain is such a highly complex dynamical system. Modern, nonlinear data analysis tools enable us to exploit the notion of recurrence in brain signal analysis. In this paper we address the analysis of electroencephalographic (EEG) data based on recurrences.

EEGs non-invasively measure small-scale changes in the brain's electric field with a high temporal resolution, which allows studying changes over time. Certain patterns of change are known to correlate with higher cognitive functions such as information processing or language comprehension. These typical patterns are called event-related potentials (ERP) and can provide valuable insights into information processing in the brain (Donchin et al., 1978). Traditionally, ERP waveforms are determined by computing an ensemble average of a large collection of EEG trials that are time-locked to a stimulus. One disadvantage of this averaging method is the high number of trials needed to reduce the signal-to-noise-ratio (Kutas and Hillyard, 1984). This is crucial for example in clinical studies, studies with children, and studies, in which repetition could influence performance. The other drawback is that such averaging implies strong assumptions on the initial state and background activities of the brain. Therefore it is strongly desirable to find new ways of analysing event-related activity on the basis of very few or even single trials.

Considering that recurrence quantification analysis (RQA) has already been applied in wide range of research fields from climate dynamics (Marwan et al., 2003), via protein sequences (Zbilut et al., 2000b), astrophysics (Kurths et al., 1994), and heart rate variability (Marwan et al., 2002), to engineering (Nichols et al., 2006), situations in which there is often only very few data available, it could be one way of achieving this.

2. Method

2.1. Recurrence plots

Recurrence is an inherent property of dynamical systems. Every such system will, given a sufficiently long time, return to an arbitrarily small neighbourhood of a previous state (Poincaré, 1890). On the basis of this fundamental property, the data analysis tool called *recurrence plot* (RP) has been devised by Eckmann et al. (1987). The RP exploits the notion of recurrence in phase space to visualise the time dependent behaviour of a dynamical system which can be pictured as a trajectory $\vec{x}(t) = \vec{x}_i \in \mathbb{R}^d$ ($i = 1, \ldots, N$, $t = i\,\Delta t$, where Δt is the sampling rate) in the d-dimensional phase space.

The main step of this visualisation is the calculation of an $N \times N$-matrix

$$\mathbf{R}_{i,j}(\varepsilon) = \begin{cases} 1: & \|\vec{x}_i - \vec{x}_j\| \leqslant \varepsilon, \\ 0: & \text{otherwise}, \end{cases} \quad \vec{x}_i \in \mathbb{R}^d, \;\; i,j = 1, \ldots, N, \tag{1}$$

where ε is a cut-off distance and $\|\cdot\|$ a norm (e.g. Euclidean or maximum norm). The crucial parameter ε defines a sphere or box centred at $\vec{x}_i$. If $\vec{x}_j$ falls within this ε vicinity, the state will be close to $\vec{x}_i$ and is considered to be a recurrence of the state $\vec{x}_i$ ($\mathbf{R}_{i,j} = 1$). The binary values in $\mathbf{R}_{i,j}$ can easily be visualised in a matrix using the colours black to denote 1 and white to denote 0 (for an illustrative example refer Fig. 1).

If only a univariate time series u_i is available, the phase space vectors x_i can be reconstructed using Taken's time delay method $\vec{x}_i = (u_i, u_{i+\tau}, \ldots, u_{i+(d-1)\,\tau})$ with embedding dimension m and delay τ (Takens, 1981). The embedding parameters can be estimated

* Corresponding author.
E-mail address: schinkel@agnld.uni-potsdam.de (S. Schinkel).

0928-4257/$ - see front matter © 2009 Elsevier Ltd. All rights reserved.
doi:10.1016/j.jphysparis.2009.05.007

using standard methods of false nearest neighbours (dimension) and mutual information (delay) (Kantz and Schreiber, 1997).

In Eq. (1) we define recurrence in terms of spatial closeness between points of phase space trajectories $\vec{x}_i$ or embedded time series u_i. We can neglect the spatial distance in phase space if we regard recurrence by using the local order structure of a trajectory. Given a univariate time series, we can start by comparing $d = 2$ time instances and define order patterns π as

$$\pi_i = \begin{cases} 0: & u_i < u_{i+\tau}, \\ 1: & u_i > u_{i+\tau}, \end{cases} \tag{2}$$

with the scaling parameter τ. *tau* ensures that the points considered in forming the order pattern π are not subject to trivial (linear) dependencies. For $d = 3$, there are six different order patterns in the triple $(u_i, u_{i+\tau}, u_{i+2\tau})$ (Fig. 2). Since tied ranks $(u_i = u_{i+\tau})$ are assumed to be rare, we neglect them. Therefore the d components in $\vec{x}_i = (u_i, u_{i+\tau}, \ldots, u_{i+(d-1)\tau})$ provide an inventory of $d!$ symbols or order patterns. With these order patterns we can form a new symbolic time series π_i and define the *order patterns recurrence plot (OPRP)* as (Groth, 2005)

$$\mathbf{R}_{i,j}(d) = \begin{cases} 1: & \pi_i = \pi_j, \\ 0: & \text{otherwise}, \end{cases} \qquad i,j = 1, \ldots, N. \tag{3}$$

The main advantage of the symbolic representation is its robustness against non-stationarity. Order patterns are invariant with respect to an arbitrary, increasing transformation of the amplitude. Furthermore, a robust complexity measure based on this symbolisation technique, the *permutation entropy*, was proposed (Bandt and Pompe, 2002) and successfully applied to epileptic seizure detection (Cao et al., 2004). Another advantage is, that the parameter space for the RQA is significantly reduced as we do not have to select a threshold ε, which cannot be estimated easily (Schinkel et al., 2008). It should be pointed out here that, strictly speaking, embedding is not necessary for the analysis of EEGs (Section 3) as the data is recorded from multiple channels which can be used instead of embedding (Thomasson et al., 2001). But by using order patterns, i.e. a symbol space, this is not possible.

2.2. Recurrence quantification analysis

A recurrence plot exhibits characteristic large-scale and small-scale patterns which are caused by typical dynamical behaviour

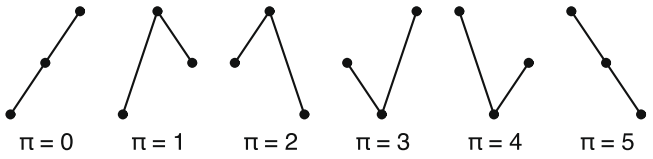

Fig. 2. Order patterns for dimension $d = 3$ (tied ranks $u_i = u_{i+\tau}$ are neglected).

(Eckmann et al., 1987; Zbilut et al., 2000a; Marwan and Kurths, 2005; Marwan et al., 2007). Depending on the nature of the underlying system, typical patterns can be observed (Fig. 3). The emergence of these structures can be used for quantifying the underlying system using a recurrence quantification analysis (RQA). In the RQA the main focus lies on the following characteristics, which we can relate to structural elements appearing in a recurrence plot (Marwan et al., 2007):

(1) *The probability that any state will recur.* This corresponds to the density of recurrence points in the RP, the *recurrence rate RR*,

$$RR = \frac{1}{N^2} \sum_{i,j} \mathbf{R}_{i,j}. \tag{4}$$

(2) *The probability that a recurrence (of any state) will further recur.* A further recurrence corresponds to segments of the phase space trajectory which run parallel for some time, i.e. the system evolves through the same states. This can be derived from an RP as the fraction of recurrence points forming diagonal line structures in the RP, the *determinism DET*,

$$DET = \frac{\sum_{l=l_{\min}}^{l_{\max}} lP(l)}{\sum_{l=1}^{l_{\max}} lP(l)}, \tag{5}$$

where $P(l)$ is the histogram of the lengths of diagonal lines. Stochastic systems have RPs with almost only single points, whereas periodic systems have RPs with very long continuous diagonal line structures. Chaotic systems usually have longer diagonal line structures but also short ones or even single points (Fig. 3). The term *determinism* is to be understood in this line of thinking.

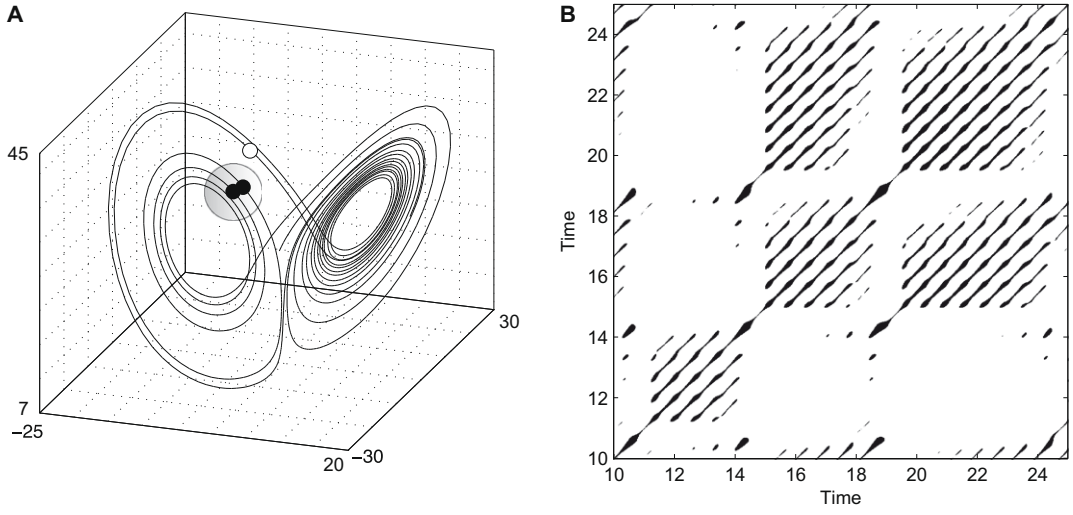

Fig. 1. The key concept of recurrence plots illustrated with a segment of the phase space trajectory of the Lorenz system (Lorenz, 1963) for standard parameters $r = 28, \sigma = 10, b = \frac{8}{3}$ (A) and its corresponding recurrence plot (B). A point of the trajectory at j which falls into the neighbourhood (grey circle in (A)) of a given point at i is considered as a recurrence point (black point on the trajectory in (A)). This is marked with a black point in the RP at the location (i, j). A point outside the neighbourhood (small circle in (A)) causes a white point in the RP.

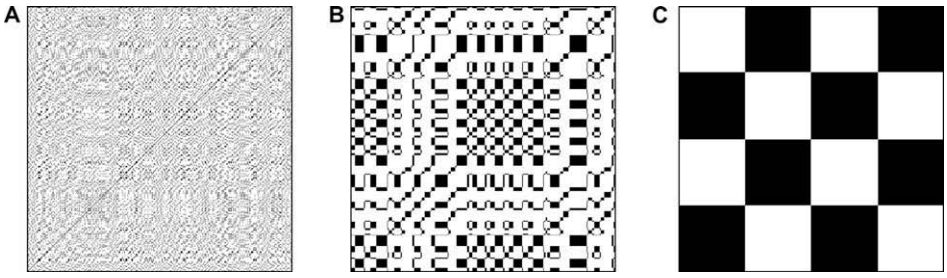

Fig. 3. Sample OPRPs of different kinds of dynamical systems. (A) white noise, (B) a chaotic system (the Lorenz system with $r = 28, b = \frac{8}{3}, \sigma = 10$) and (C) a periodic signal (sine wave). The embedding parameters were $m = 3, \tau = 3$ (A and C) and $m = 3, \tau = 15$ (B).

(3) *The mean and maximal duration of recurrences of any states.* This is the length of the parallel-running of close phase space trajectories and corresponds to the *mean and maximal length* of diagonal line structures appearing in the RP,

$$\langle L \rangle = \frac{\sum_{l=l_{\min}}^{l_{\max}} lP(l)}{\sum_{l=l_{\min}}^{l_{\max}} P(l)}. \quad (6)$$

These lengths can also be understood as a measure for predictability of the system or divergence of states. The higher the maximal positive Lyapunov exponent of the system, the shorter the duration of recurrences, thus of these line lengths. In fact, it can be shown that the line lengths of the diagonal structures are directly related to the K_2 entropy, which is the lower limit of the sum of the positive Lyapunov exponents (Thiel et al., 2004).

(4) *The uncertainty of the knowledge that the system will further recur.* This is an information measure and corresponds to the *Shannon entropy* of the probability distributions of the diagonal line structures in the RP,

$$ENT = -\sum_{l=l_{\min}}^{l_{\max}} p(l) \ln p(l) \quad \text{with } p(l) = \frac{P(l)}{\sum_{l=l_{\min}}^{l_{\max}} P(l)}. \quad (7)$$

These measures can be computed from the whole RP or in moving windows (i.e. sub-RPs) moved along the main diagonal of the RP. The latter allows studying changes of these measures in time, which can reveal transitions in the system (Trulla et al., 1996). Despite the valuable knowledge about dynamical systems these complexity measures can provide, they can also be used to discriminate experimental conditions in cognitive science.

3. Material – semantic mismatch (N400)

The paradigm used here was first introduced by (Kutas and Hillyard, 1980) and features an N400, a negative deflection in the EEG, when processing semantically anomalous sentences in comparison to their semantically correct counterparts (Table 1).

3.1. Subjects and procedure

We re-analyse data that has already been analysed by Allefeld et al. (2005). 16 subjects (eight female) participated in a language processing study. All were right-handed, monolingual native speakers of German aged 20–27. The stimulus material was presented in a word-by-word fashion on a 17 in. computer screen. The language material consisted of 52 pairs of sentences (Table 1). From correct german sentences (C50) semantically mismatching counterparts (C51) were constructed by exchanging the terminal verbs. Words were presented for 400 ms each with an interstimulus interval of 100 ms. A probe word was presented 800 ms after the last item. Subjects had to indicate whether the probe word had occured in the given form in the preceding sentence by pressing a button within 3.5 s. This ensured that subjects had perceived the sentence correctly. The probe words were either the verb or the noun of the preceding sentence or a semantically related alternative. The probe items were balanced for correctness and word category. After a pause of 1 s the next trial started. Subjects had to read a total of 104 sentences in each condition. The EEG was recorded with a sampling rate of 250 Hz from 59 Ag/AgCl scalp electrodes (impedances $\leqslant$ 5 kΩ). The Electrooculogram (EOG) was monitored to scan for artifacts. If the subject had answered the probe question correctly, artifact-free epochs from −600 to 1300 ms relative to the critical verb entered further analysis.

3.2. Data analysis

In this example we used order patterns recurrence plots as defined in Eq. (3). For the OPRPs of the EEG measurements the necessary time delay τ was determined channelwise using the mutual information (Roulston, 1999). The estimated delay typically ranged from 8 to 10 and we used the mode, $\tau = 9$, as a fixed τ for all successive analysis. The number of considered time instances d was 3. The RQA was computed in sliding windows with a size of 60 data points (240 ms) and shifted by 1 data point (4 ms). For plotting and further analysis we aligned time to the centre of the moving window. Note that contrary to the usual procedure we neither baseline-aligned nor re-referenced the data, which is a prequesite for the traditional ERP analysis.

4. Results

For a first impression we visually inspected the temporal evolution of the complexity measures in condition C50 and C51. In the semantic mismatch condition C51, numerous transitions in the critical time window of 300—600 ms post-stimulus could be found for a variety of RQA measures (Fig. 4 (B, D, and F)), whereas transitions are hardly observable in the control condition (Fig. 4 (A, C, and E)).

Table 1
Sample sentences used in the experiment described. Sentences like C51 elicit a negative going waveform in the EEG relative to a control sentence Kutas and Hillyard, 1980.

	Condition	Example
C50	Control	Das Holz wurde gesägt (*The timber was sawn*)
C51	Semantic mismatch	Das Holz wurde zitiert (*The timber was quoted*)

As the aim of this paper is to show the real life applicability of the method, we will focus on the simplest RQA measure, *RR*, for further analysis. Even though other RQA measures also serve as indicators (Fig. 4), they are not necessary for the purpose at hand, the discrimination of experimental conditions. Further we consciously focus on single trials. The paradigm used is well-known and the existence of the N400 component is not in question (Kutas and Hillyard, 1980). We want to show that the method is capable of detecting the component in individual single channel measurements. Therefore, we will compare the performance of *RR* to that of voltage measurements in terms of single trials. The procedure for this is as follows: we estimate the 95% confidence interval (CI) of the control condition C50 to which we then compare the single trials of the experimental condition C51. For the estimation of the CIs we use all measurements of one channel in the control condition separately for each subject. Using *RR* we can easily discriminate condition C51 from the control condition C50 (Fig. 5, left column) in single trials. This pattern is consistent across subjects (4 shown here). For exactly the same trials this discrimination is not possible when using the voltage

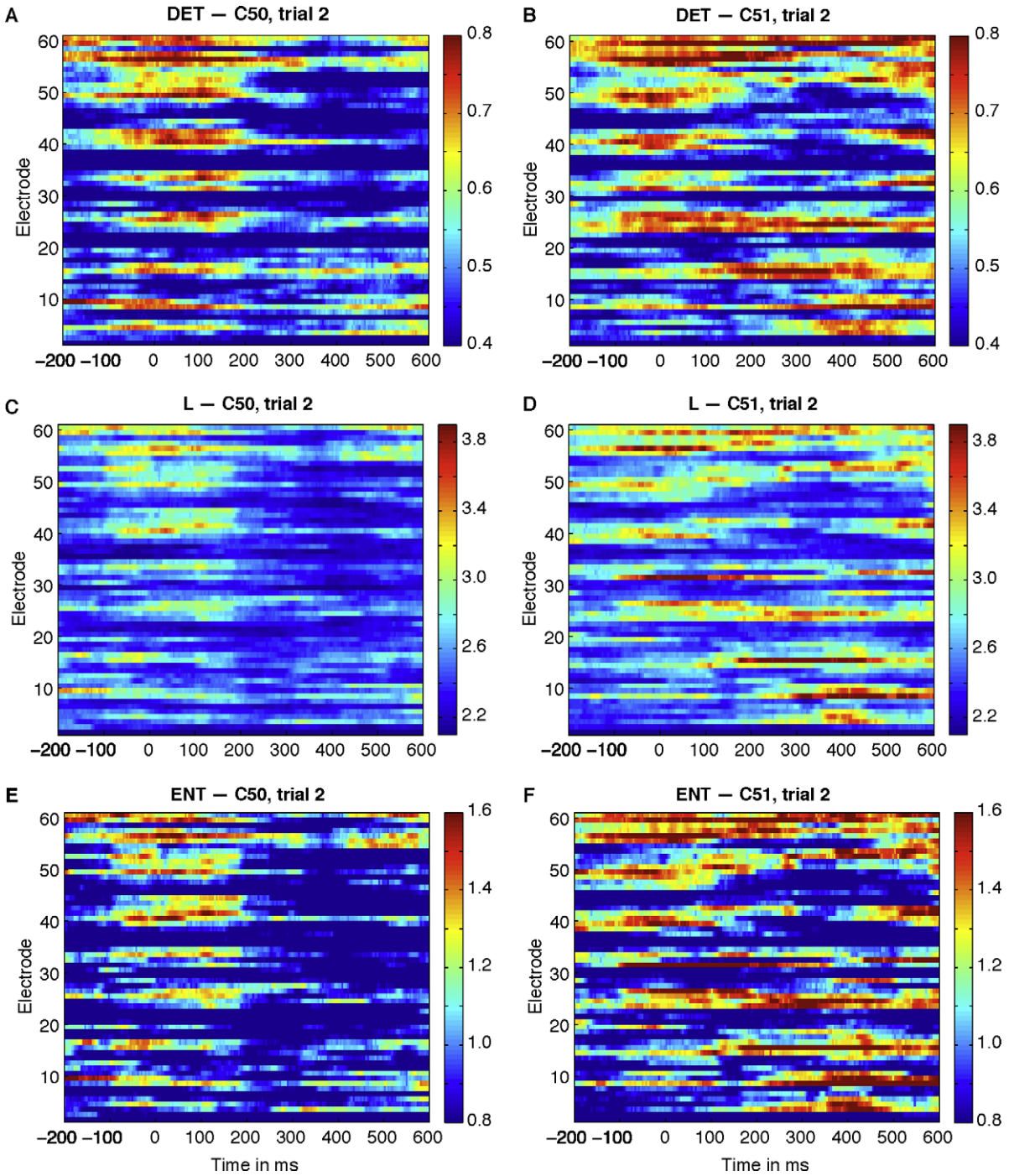

Fig. 4. Temporal evolution of chosen RQA measures in condition C50 and C51 in a representative trial (trial 2) at all electrode sites. In condition C51 (Fig. 4 (B, D, and F)) numerous transitions between 300 and 600 ms are found while the control condition C50 lacks these (Fig.4 (A, C, and E)).

measurements. The single trials do not leave the CI of the control conditions (Fig. 5, right column). Note that the recurrence based method is indeed only sensitive to the ERP effect. The measures do not significantly deviate from the control condition apart from the time window which is known to reflect the N400 component (300—600 ms). Furthermore, the RQA based analysis very cleary shows that the N400 is not stable in time, the well-known *latency-jitter*, which is present in all subjects but strongly varies across subjects. This is problematic when averaging the data since re-aligning the timescale is not trivial and might lead to spurious or even wrong results.

We analysed the performance of the EEG voltage measurements and *RR* in these comparisons (Fig. 5) on nine electrode sites (F7, FZ, F8, P7, CZ, P8, PO3, PZ, PO4) individually for each subject yielding a total of 14,256 comparisons. The outcome was classified into three groups. A comparison was classified as right if the experimental condition left the CI of the reference condition only within the expected time window (300—600 ms) for at least 10 epochs (40 ms). If the experimental condition left the CI outside the expected time window for too long, 50 epochs (200 ms) consecutive or in total, the comparison was classified as wrong. In the case of the EEG data a comparison was also classified as wrong if the CI was left in the wrong direction i.e. detection of a P-Effect instead of an N-Effect. For the *RR* this was not necessary as the behaviour was consistent such that *RR* was either higher in the experimental condition or not outside the CI at all. If the CI was not left at all, the trial was counted as not classifiable (none). A summary of the analysis is given in Table 2. A detailed list split by subjects and electrodes is given in Table 3 in the Appendix A.

The overall ability to classify the trials at all is rather poor in both cases, 12.7% for EEG and 14.2% for *RR*. This is not

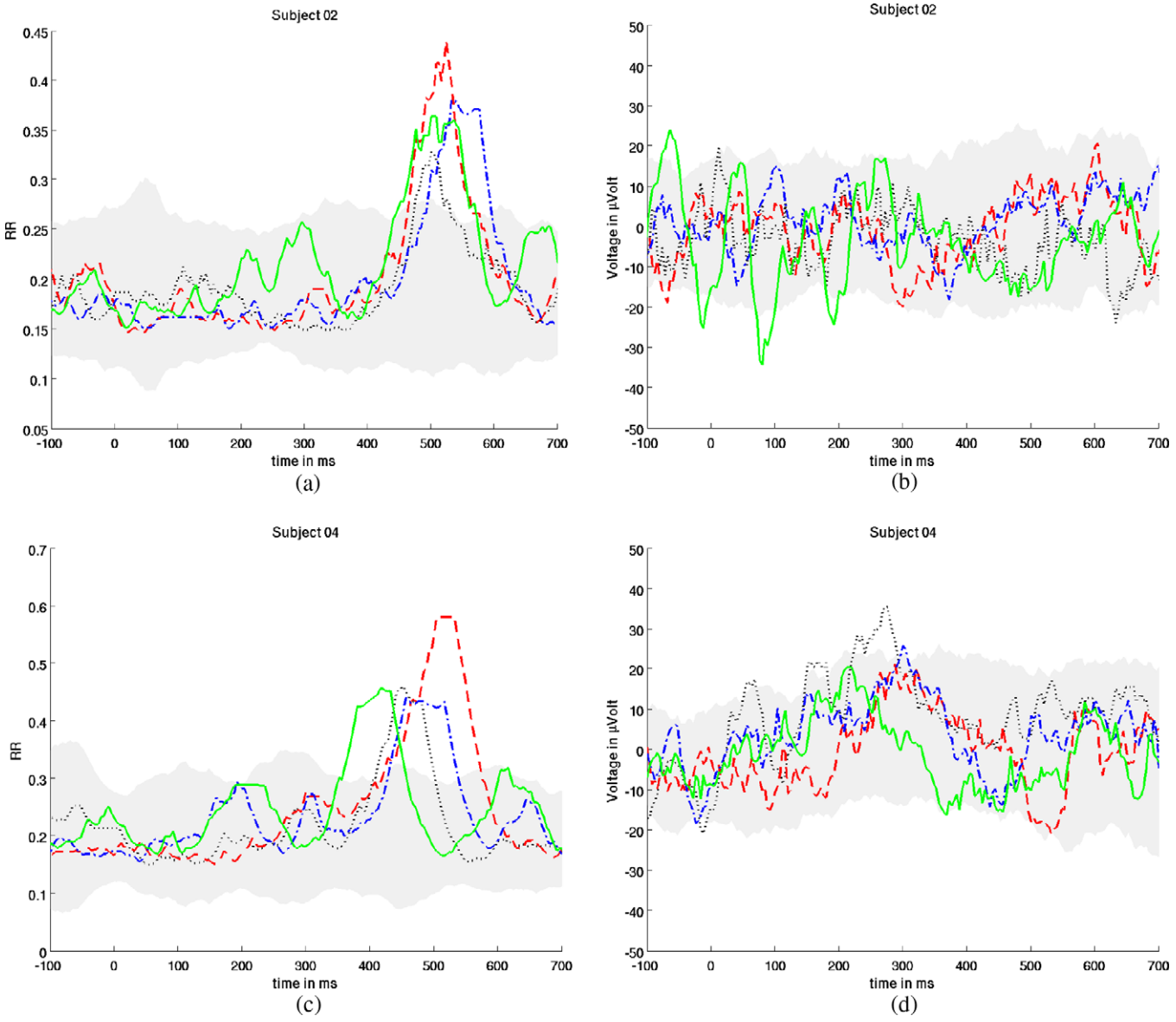

Fig. 5. Comparison of single trials (coloured lines) in experimental condition C51 versus the averaged control condition C50 at CZ. *RR* (left column) and voltage measurements (right column) for four subjects. The shaded area denotes the 95% confidence interval of the control condition. The trials in the left and the right column are identical (colour and line-style matched). (For interpretation of the references to colour in this figure legend, the reader is referred to the web version of this article.)

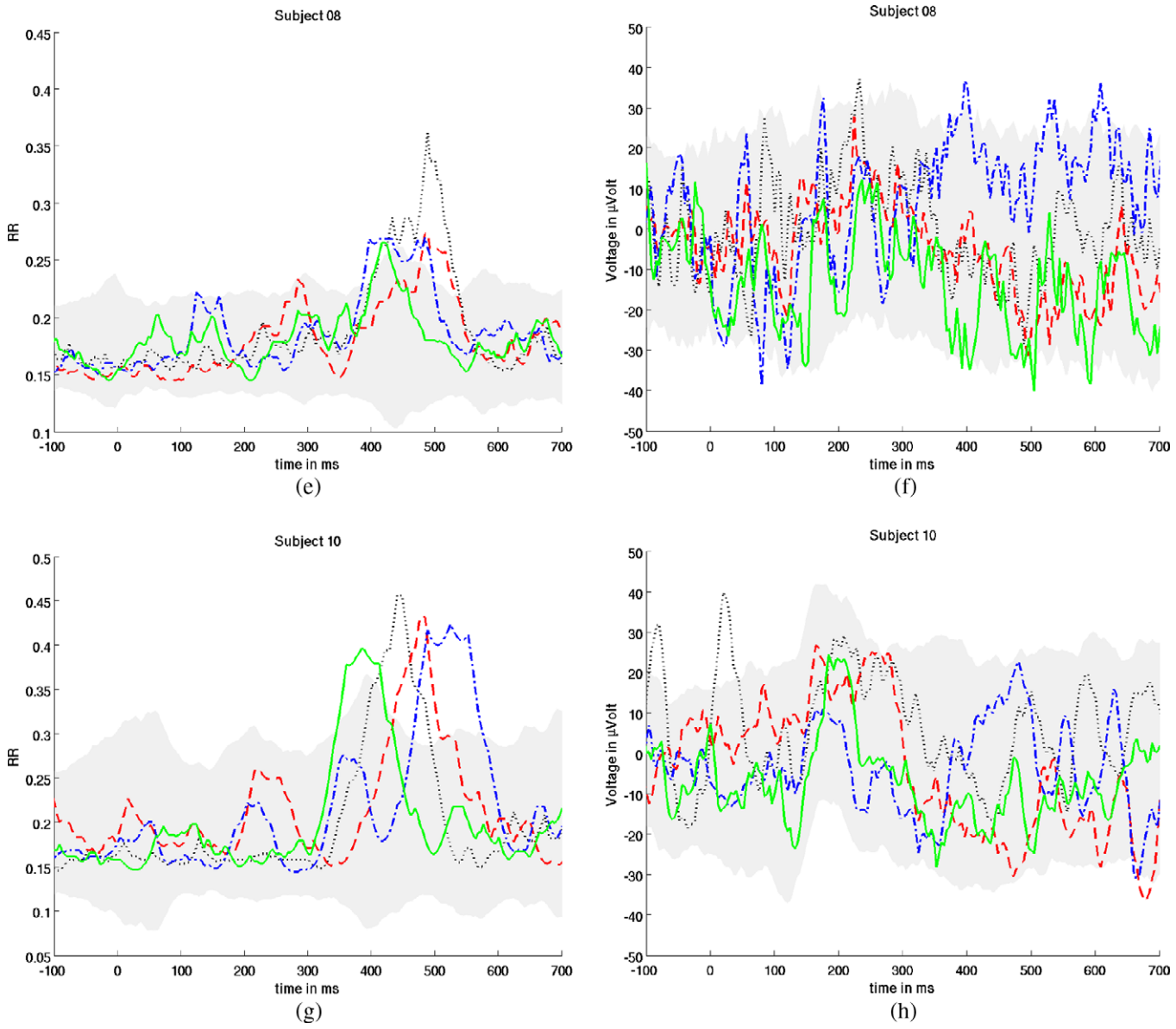

Fig. 5 (*continued*)

surprising given the difficulty of the task. Yet there is one important difference. The vast majority of trials that could be classified are classified properly when using *RR*. When using the voltage measurements the situation is reversed. While only $\sim 1.5\%$ of trials is classified correctly about seven times as many trials are classified wrongly. This is a strong indication that the recurrence based method is more powerful in terms of single trial classification as not even a quarter of a percent is classified wrongly.

Table 2
Overall performance of the the EEG voltage measurements and the RQA measure *RR* in terms of single trial comparisons analogue to Fig. 5. *RR* is outperforming the voltage measurements in terms of overall ability to classify and more importantly in correct classification. A detailed list splitted by subjects and electrodes is given in Appendix A.

Measure	Right (%)	None (%)	Wrong (%)
EEG	1.45	88.26	10.29
RR	14.02	85.77	0.22

5. Summary and discussion

We have presented a method for brain signal analysis that rests on the natural property of recurrence in dynamical systems. In the present case recurrence was defined in terms of a trajectory's local rank structure. This rank structure is symbolically endoded as order patterns. The main advantage of our approach is that it rests on very few assumptions. It can be used as a diagnostical tool without requiring any knowledge about the generation of an ERP. The other major advantage of the method presented is, that it can detect well-known ERP components, in our case the N400, even on the scale of single measurements. A significant advance compared to the traditional averaging method.

Given the promising results of the single trial analysis presented here, our current research is aimed at studying the functional connectivity deriveable from EEG data by means of recurrence quantification analysis (RQA). As the complexity measures obtained by the RQA are very sensitive to event-related activity we expect to be able to extract consistent patterns of connectivity on the basis of very few or even single trials.

Table 3
Single-trial comparisons by subject and electrode site for the EEG voltage measurements and the RQA measure *RR*.

Subject	Electrode	Right (EEG)	None (EEG)	Wrong (EEG)	Right (RR)	None (RR)	Wrong (RR)
01	F7	2	81	13	11	85	0
01	FZ	1	84	11	23	73	0
01	F8	0	83	13	15	81	0
01	P7	1	79	16	15	81	0
01	CZ	1	84	11	22	74	0
01	P8	2	72	22	14	82	0
01	PO3	0	81	15	10	86	0
01	PZ	5	82	9	8	87	1
01	PO4	4	74	18	10	86	0
02	F7	2	96	2	10	90	0
02	FZ	5	84	11	11	89	0
02	F8	2	90	8	17	83	0
02	P7	1	94	5	23	76	1
02	CZ	2	90	8	16	84	0
02	P8	3	87	10	12	87	1
02	PO3	2	89	9	15	85	0
02	PZ	1	89	10	10	89	1
02	PO4	2	86	12	10	90	0
03	F7	3	81	13	20	77	0
03	FZ	1	90	6	14	83	0
03	F8	2	91	4	7	90	0
03	P7	2	80	15	18	79	0
03	CZ	1	86	10	19	78	0
03	P8	1	85	11	15	82	0
03	PO3	7	75	15	16	81	0
03	PZ	1	86	10	21	76	0
03	PO4	4	79	14	24	73	0
04	F7	1	95	7	14	88	1
04	FZ	3	83	17	12	91	0
04	F8	3	87	13	11	92	0
04	P7	2	93	8	16	87	0
04	CZ	1	90	12	16	87	0
04	P8	4	91	8	13	90	0
04	PO3	5	83	15	20	83	0
04	PZ	1	92	10	20	83	0
04	PO4	2	87	14	18	85	0
05	F7	0	86	9	15	80	0
05	FZ	3	80	12	16	79	0
05	F8	4	77	14	17	77	1
05	P7	2	69	24	3	92	0
05	CZ	1	84	10	14	80	1
05	P8	0	87	8	6	89	0
05	PO3	1	84	10	14	81	0
05	PZ	1	85	9	5	90	0
05	PO4	2	74	19	7	88	0
06	F7	0	90	10	13	85	2
06	FZ	0	91	9	21	79	0
06	F8	0	96	4	13	87	0
06	P7	0	90	10	10	89	1
06	CZ	0	92	8	21	79	0
06	P8	1	89	10	13	87	0
06	PO3	0	90	10	13	87	0
06	PZ	1	89	10	16	84	0
06	PO4	0	91	9	18	82	0
07	F7	1	92	7	17	83	0
07	FZ	5	81	14	14	85	1
07	F8	3	87	10	12	88	0
07	P7	2	89	9	19	81	0
07	CZ	3	86	11	16	84	0
07	P8	1	89	10	21	78	1
07	PO3	5	82	13	24	76	0
07	PZ	2	76	22	13	87	0
07	PO4	3	86	11	21	79	0
08	F7	0	89	10	6	93	0
08	FZ	0	91	8	10	89	0
08	F8	0	93	6	11	88	0
08	P7	2	94	3	5	94	0
08	CZ	0	87	12	9	89	1
08	P8	0	93	6	7	92	0
08	PO3	0	94	5	8	91	0
08	PZ	1	91	7	5	94	0
08	PO4	1	92	6	8	91	0
10	F7	0	94	5	20	78	1
10	FZ	3	85	11	14	85	0

(*continued on next page*)

Table 3 (*continued*)

Subject	Electrode	Right (EEG)	None (EEG)	Wrong (EEG)	Right (RR)	None (RR)	Wrong (RR)
10	F8	0	91	8	11	88	0
10	P7	7	83	9	17	80	2
10	CZ	1	90	8	13	86	0
10	P8	4	78	17	12	87	0
10	PO3	5	79	15	14	84	1
10	PZ	5	82	12	19	79	1
10	PO4	6	78	15	15	83	1
11	F7	2	85	11	10	88	0
11	FZ	1	85	12	19	79	0
11	F8	0	94	4	22	76	0
11	P7	0	93	5	13	85	0
11	CZ	1	89	8	15	83	0
11	P8	0	91	7	13	85	0
11	PO3	1	86	11	19	78	1
11	PZ	1	90	7	15	83	0
11	PO4	2	90	6	16	82	0
12	F7	2	90	10	17	85	0
12	FZ	2	84	16	12	90	0
12	F8	0	90	12	5	97	0
12	P7	0	87	15	5	97	0
12	CZ	2	85	15	12	89	1
12	P8	1	78	23	7	95	0
12	PO3	0	91	11	12	89	1
12	PZ	0	85	17	12	90	0
12	PO4	1	85	16	5	97	0
13	F7	3	87	11	13	88	0
13	FZ	0	95	6	7	94	0
13	F8	2	91	8	14	87	0
13	P7	1	82	18	14	87	0
13	CZ	2	86	13	17	84	0
13	P8	3	80	18	9	92	0
13	PO3	2	81	18	8	93	0
13	PZ	0	97	4	17	84	0
13	PO4	4	83	14	13	88	0
14	F7	0	89	9	10	87	1
14	FZ	1	89	8	20	78	0
14	F8	0	92	6	14	84	0
14	P7	1	90	7	16	81	1
14	CZ	0	89	9	16	82	0
14	P8	0	88	10	17	80	1
14	PO3	0	91	7	17	81	0
14	PZ	0	91	7	13	85	0
14	PO4	0	90	8	14	84	0
15	F7	0	89	5	21	73	0
15	FZ	0	90	4	17	77	0
15	F8	0	89	5	10	84	0
15	P7	1	88	5	17	77	0
15	CZ	1	86	7	16	78	0
15	P8	0	90	4	13	81	0
15	PO3	0	87	7	13	81	0
15	PZ	1	88	5	16	78	0
15	PO4	0	88	6	11	83	0
16	F7	0	93	9	12	90	0
16	FZ	3	95	4	20	81	1
16	F8	0	100	2	13	89	0
16	P7	1	94	7	14	87	1
16	CZ	1	92	9	16	86	0
16	P8	0	94	8	12	90	0
16	PO3	1	92	9	19	83	0
16	PZ	3	90	9	20	81	1
16	PO4	1	87	14	14	88	0
17	F7	0	92	8	12	87	1
17	FZ	0	89	11	7	93	0
17	F8	0	94	6	5	94	1
17	P7	0	87	13	14	86	0
17	CZ	1	92	7	7	93	0
17	P8	1	91	8	14	85	1
17	PO3	1	84	15	12	88	0
17	PZ	0	86	14	16	84	0
17	PO4	0	91	9	17	83	0

Acknowledgements

We thank C. Allefeld, S. Frisch and M. Schlesewsky for providing the EEG data of the experiment. This work was supported by grants of the European Union through the Network of Excellence BioSim, contract LSHB-CT-2004-005137 and No. 65533 and the COST Action BM0601 *NeuroMath: Advanced Methods For The Estimation Of Human Brain Activity And Connectivity*, and by the German Science

Foundation (DFG) in the SFB 555 *Komplexe nichtlineare Systeme*, the Research Group FG 868: *Computational Modeling of Behavioral, Cognitive and Neural Dynamics*. The software used for this paper is available for download at http://tocsy.agnld.uni-potsdam.de.

Appendix A

A.1. Detailed single-trial comparisons

See Table 3.

References

Allefeld, C., Frisch, S., Schlesewsky, M., 2005. Detection of early cognitive processing by event-related phase synchronization analysis. Neuroreport 16 (1), 13–16.
Bandt, C., Pompe, B., 2002. Permutation entropy – a complexity measure for time series. Physical Review Letters 88, 174102.
Cao, Y., Tung, W., Gao, J.B., Protopopescu, V.A., Hively, L.M., 2004. Detecting dynamical changes in time series using the permutation entropy. Physical Review E 70, 046217.
Donchin, E., Ritter, W., McCallum, C., 1978. Cognitive psychophysiology: the endogenous components of the ERP. In: Callaway, E., Tueting, P., Koslow, S. (Eds.), Event-Related Potentials in Man. Academic Press, New York, pp. 349–441.
Eckmann, J.-P., Kamphorst, S.O., Ruelle, D., 1987. Recurrence plots of dynamical systems. Europhysics Letters 5, 973–977.
Groth, A., 2005. Visualization of coupling in time series by order recurrence plots. Physical Review E 72 (4), 046220.
Kantz, H., Schreiber, T., 1997. Nonlinear Time Series Analysis. University Press, Cambridge.
Kurths, J., Schwarz, U., Sonett, C.P., Parlitz, U., 1994. Testing nonlinearity in radiocarbon data. Nonlinear Processes in Geophysics 1 (1), 72–75.
Kutas, M., Hillyard, S., 1980. Reading senseless sentences: brain potentials reflect semantic incongruity. Science 207, 203–204.
Kutas, M., Hillyard, S., 1984. Brain potentials during reading reflect word expectancy and semantic association. Nature 307, 161–163.
Lorenz, E.N., 1963. Deterministic nonperiodic flow. Journal of the Atmospheric Sciences 20, 120–141.
Marwan, N., Kurths, J., 2005. Line structures in recurrence plots. Physics Letters A 336 (4–5), 349–357.
Marwan, N., Wessel, N., Meyerfeldt, U., Schirdewan, A., Kurths, J., 2002. Recurrence plot based measures of complexity and its application to heart rate variability data. Physical Review E 66 (2), 026702.
Marwan, N., Trauth, M.H., Vuille, M., Kurths, J., 2003. Comparing modern and Pleistocene ENSO-like influences in NW Argentina using nonlinear time series analysis methods. Climate Dynamics 21 (3–4), 317–326.
Marwan, N., Romano, M.C., Thiel, M., Kurths, J., 2007. Recurrence plots for the analysis of complex systems. Physics Reports 438 (5–6), 237–329.
Nichols, J.M., Trickey, S.T., Seaver, M., 2006. Damage detection using multivariate recurrence quantification analysis. Mechanical Systems and Signal Processing 20 (2), 421–437.
Poincaré, J., 1890. Sur le probléme des trois corps et les équations de la dynamic. Acta Mathematica 13, 1–270.
Roulston, M.S., 1999. Estimating the errors on measured entropy and mutual information. Physica D: Nonlinear Phenomena 125, 285–294.
Schinkel, S., Dimigen, O., Marwan, N., 2008. Selection of recurrence threshold for signal detection. European Physics Journal – Special Topics 164, 45–53.
Takens, F., 1981. Detecting strange attractors in turbulence. Lecture Notes in Mathematics 898 (1), 366–387.
Thiel, M., Romano, M.C., Read, P.L., Kurths, J., 2004. Estimation of dynamical invariants without embedding by recurrence plots. Chaos 14 (2), 234–243.
Thomasson, N., Hoeppner, T.J., Webber Jr., C.L., Zbilut, J.P., 2001. Recurrence quantification in epileptic EEGs. Physics Letters A 279 (1–2), 94–101.
Trulla, L.L., Giuliani, A., Zbilut, J.P., Webber Jr., C.L., 1996. Recurrence quantification analysis of the logistic equation with transients. Physics Letters A 223 (4), 255–260.
Zbilut, J.P., Giuliani, A.L., Webber Jr., C., 2000a. Recurrence quantification analysis as an empirical test to distinguish relatively short deterministic versus random number series. Physics Letters A 267 (2–3), 174–178.
Zbilut, J.P., Webber Jr., C.L., Colosimo, A., Giuliani, A., 2000b. The role of hydrophobicity patterns in prion folding as revealed by recurrence quantification analysis of primary structure. Protein Engineering 13 (2), 99–104.